Process-Resolved Morphology of Bismaleimide Matrix Composites

JEAN-FRANÇOIS VIOT* and JAMES C. SEFERIS,† *Polymeric Composites Laboratory, Department of Chemical Engineering, University of Washington, Seattle, Washington 98195*

Synopsis

A series of silicone-modified bismaleimide resins have been examined as matrices for high performance continuous fiber-reinforced composite materials. Detailed studies of the interrelation between processing, structure, and properties of both the neat resin and corresponding carbon-fiber-reinforced composite have identified that the silicone additive provides important morphological modification to the bismaleimide matrix for toughness improvements while, at the same time, retaining the elevated temperature performance. Micrographs of fracture surfaces of cured samples demonstrate remarkable similarities to fracture surfaces of rubber-modified epoxy matrices. Specifically, a fracture surface covered with noncommunicating microcavities of 1.5 μm in diameter was observed. However, unlike rubber-modified epoxies where the observed features are assumed to be created during fracture of the specimen, this study demonstrates that the microcavities are created during the cure process and, thus, exist in the bulk of the material before fracture. In simulated cures of the material either while observed directly in a polarizing microscope or indirectly inside thermal analysis cells (DSC, TGA) and with examination of fractured surfaces of samples cured according to different temperature profiles, it is established that the silicone modifier, in conjunction with the processing conditions, is responsible for the morphological developments. Accordingly, a mechanism describing the observed morphology was proposed based on physical changes that the silicone additive experiences in relation to specific volatile products emitted during the cure process.

INTRODUCTION

Polyimide resin matrices offer an increase in use temperature of structural composites over the traditionally used epoxy-based matrices.[1-3] However, the exceptionally high thermooxidative stability of wholly aromatic polyimides is countered by their difficult processability which involves a mixture of monomers in a low boiling point alcohol. The solvent impregnation route has the familiar problem in creating microcracked composites. An alternate to solution impregnation has been the creation of a polyaddition route of short preimidized segments which then, with other additives, offers a melt-impregnation route similar to epoxy matrices. Bismaleimide-based resins are by far the more widely used materials following this route. The high functionality combined with the short length of the monomer leads to a very dense crosslinked network. High stiffness but also undesired brittleness result from this molecular structure. One means to overcome this drawback is to copo-

*Present address: Rhone-Poulenc Recherches, Centre Des Carrieres, B. P. 62, 69192 Saint-Fons Cedex, France.

†Author to whom correspondence should be addressed.

Journal of Applied Polymer Science, Vol. 34, 1459–1475 (1987)
 CCC 0021-8995/87/041459-17$04.00

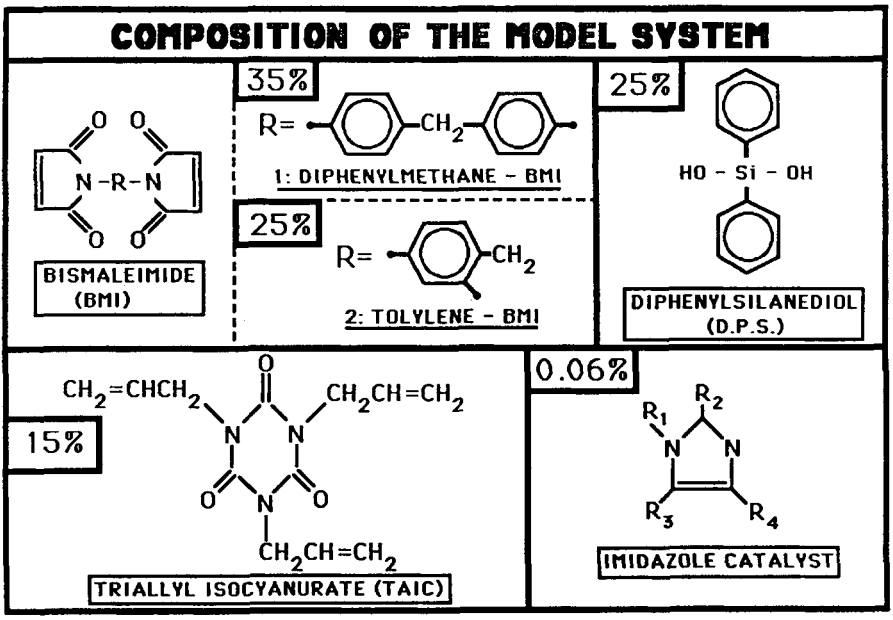

Fig. 1. Components of the Kerimid FE 70003 model bismaleimide formulation.

lymerize the bismaleimide with long chains or oligomers to loosen the network; it is also possible to add a component creating an interpenetrating network with increased toughness. The development of a two-phase system proved to decrease inherent brittleness of bismaleimide resins as well.[1]

A resin system based on bismaleimide chemistry and modified with a silicone monomer, diphenylsilanediol, is investigated in this work as a model high temperature system.[2] This work forms an important addition to our overall developing methodology for interrelating processing, structure, and properties of polymer composites, in general, and polyimide-based composites, in particular.[3-5] For the bismaleimide system examined in this work, a specific morphology induced by the inclusion of diphenylsilanediol as the modifier was identified and its creation observed in relation to the processing conditions employed during the cure both for the neat resin and carbon-fiber-reinforced composites.

EXPERIMENTAL

Materials and Processing

The model bismaleimide examined in this work, as well as the individual constituents, was made available by Rhone-Poulenc, Inc. The system was based on the Kerimid family whose components are shown in Figure 1. The model formulation Kerimid FE 70003, which has also been examined in other studies as well, formed the base system.[7] Its composition (by wt %) is diphenylmethane BMI (35%), tolylene BMI (25%), triallylisocyanurate or TAIC (15%), diphenylsilanediol or DPS (25%), and imidazole (0.06%), which catalyzes the BMI polymerization and crosslinking. A basic cure cycle for laminating prepregs of carbon fibers has been developed in a previous part of

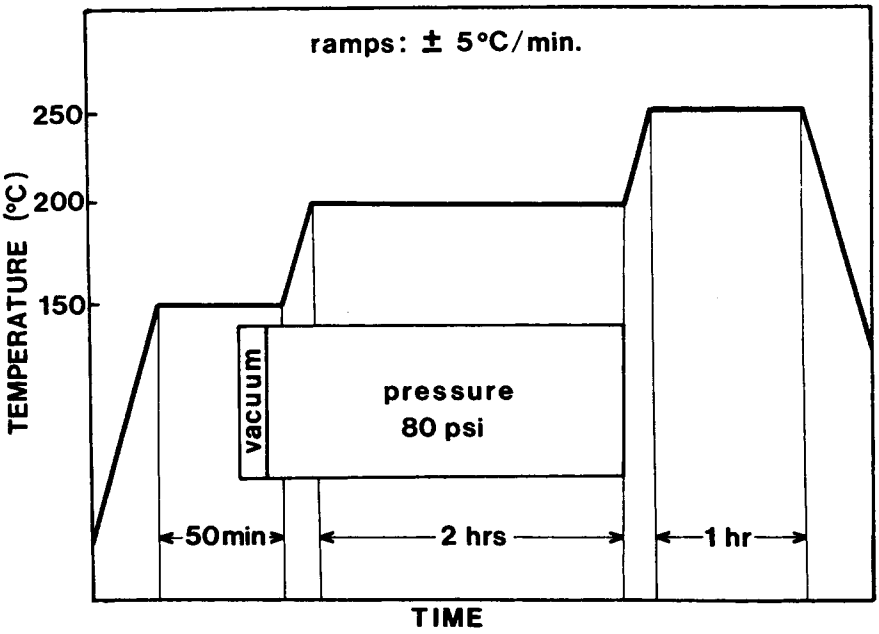

Fig. 2. Cure cycle established for the Kerimid FE 70003 model formulation.

our overall program based on thermal and rheological analyses.[8] This cure cycle is summarized in Figure 2. Neat resin plaques were cast under atmospheric pressure, following the same temperature profile as for the composite lamination. Specifically, the prepolymer was degassed in a beaker under vacuum until 10 min before the end of the first plateau at 150°C. At that time, the resin was poured into a preheated vertical mold made of two glass plates separated by a U-shaped piece of Teflon of approximately 4–8 mm thickness. This mold setup allows for easy degassing of volatile products since the top surface of the sample is always in contact with air during the cure. Vacuum was applied for 5 additional minutes and stopped until the end of the cure. For comparison, a formulation without diphenylsilanediol (i.e., diphenylmethane BMI 47%, tolylene BMI 33%, TAIC 20%, imidazole 0.06%) was also cured following the same cure process. Pure DPS was also examined. Finally, in order to establish the presence of DPS in the observed morphology of the basic formulation, fractured samples were immersed for 10 min in hexafluoropropanol, which is a swelling solvent for DPS. Finally, composite samples utilizing the same cure cycle were made with the basic bismaleimide formulation.

Morphological and Thermal Evaluations

Cured samples were fractured in liquid nitrogen and at room temperature. The fracture surfaces were gold plated (about 200 Å by sputtering) and examined in a scanning electron microscope (ISI MSM-5 "mini SEM"). Fracture surfaces were generated perpendicularly to the free top surface of the sample; and regions close to the top were examined in order to investigate skin effects.

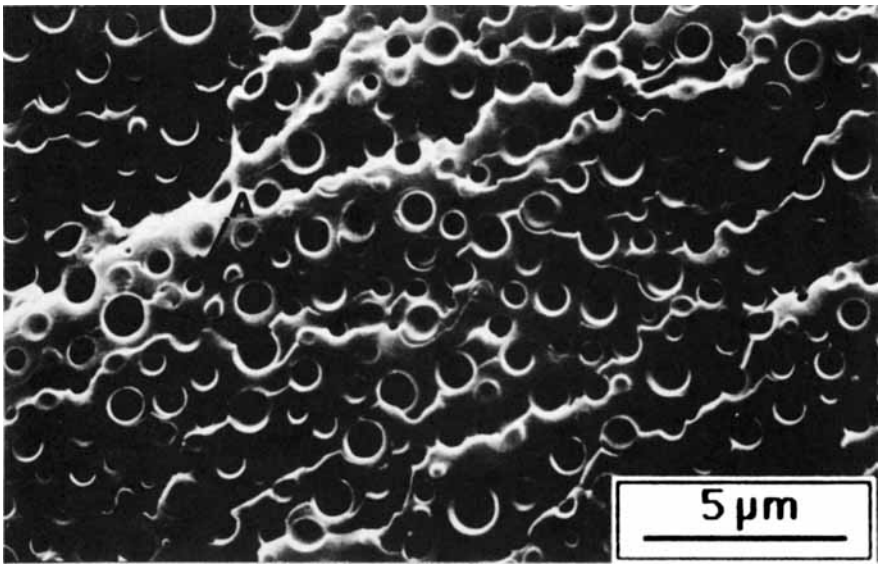

Fig. 3. Fracture surface of the cured model system. The sample was fractured at room temperature. The fracture surface is covered with noncommunicating microcavities 1.5 μm in diameter.

Morphological changes in the curing resin were observed in real time by transmission optical microscopy through a sample of model prepolymer sprayed out in its molten state on a glass slide to form a wide drop about 20 μm in thickness and 10 mm in diameter. The glass slide was placed on a programmable heated stage (Linkam TH 600 and PR600) simulating the cure cycle. The Nikon polarizing microscope used in this study was also equipped with an on-line video recorder.

Finally, thermal analyses of all systems examined were performed with a Dupont System 9900 operating DSC, TGA, TMA, and DMA modules.

RESULTS AND DISCUSSION

Definition of the Morphology

A typical fracture surface micrograph of the model bismaleimide system examined is shown in Figure 3. As can be seen, the surface is covered by what appears to be microcavities of approximately 1.5 μm in diameter. This observed morphology is quite similar to the one observed with some rubber-modified epoxy fracture surfaces, where it is hypothesized that it is created during the fracture process. This morphology is thought to arise from either cavitation, crazing, or debonding of the rubber particles that were phase separated during the cure of the sample.[9-13]

In order to verify that here, too, the DPS modifier is responsible for the observed cavities, a fracture surface was generated on a sample cured from the nonmodified formulation (BMI + TAIC + catalyst). As can be seen in Figure 4, such a fracture surface appears totally cavity-free at the same magnification as the system with the DPS exhibiting cavities.

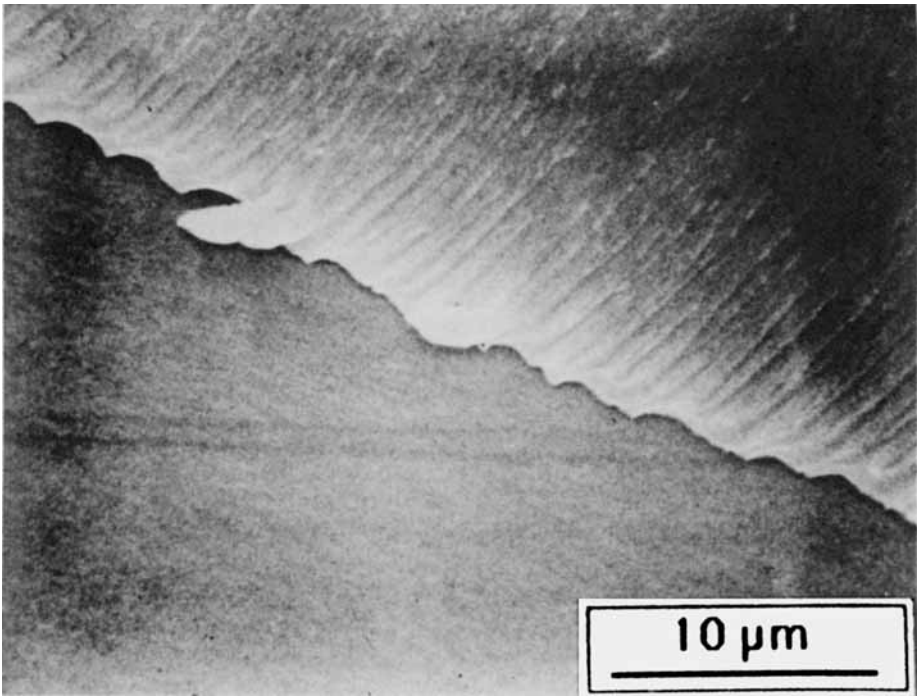

Fig. 4. Fracture surface of the cured nonmodified resin. The sample was fractured at room temperature. No cavities are detectable.

However, contrary to the modified epoxy systems, it was observed, as in Figure 5, that the fracture surface aspect did not change when the sample was fractured in liquid nitrogen (−196°C). This observation suggests that the cavities may be formed during processing and, therefore, are part of the bulk of the material. Indeed, at −196°C, both bismaleimide and DPS are extremely brittle. As a consequence, any mechanism involving permanent strain at the fracture tip is highly questionable. This would be the case for both cavitation (strain of a DPS particle assumed to occupy the cavity before fracture) and crazing (strain of the resin around the same kind of particle). Debonding between the resin and precipitated particles is then the only remaining possible mechanism for creating cavities during fracture. If so, debonding would occur at a 100% rate since no particle can be detected in any of the cavities, possible only if no adhesion exists between the resin and the precipitated material; even repulsion between these two entities would be necessary for such an event. However, debonding may be refuted by the observation of cavities located slightly beneath the fracture surface which are only opened at their top by the fracture. These cavities appear to be empty, too. For clarity, one of these cavities is highlighted as A in Figure 3.

For more evidence of the existence of the cavities in the material before fracture, densities of the model system as well as its major constituents (BMI + TAIC) and DPS were compared before and after cure. The results are presented in Table I. It appears that the densities of the two constituents of the model resin increase during the cure, while the density of the model resin

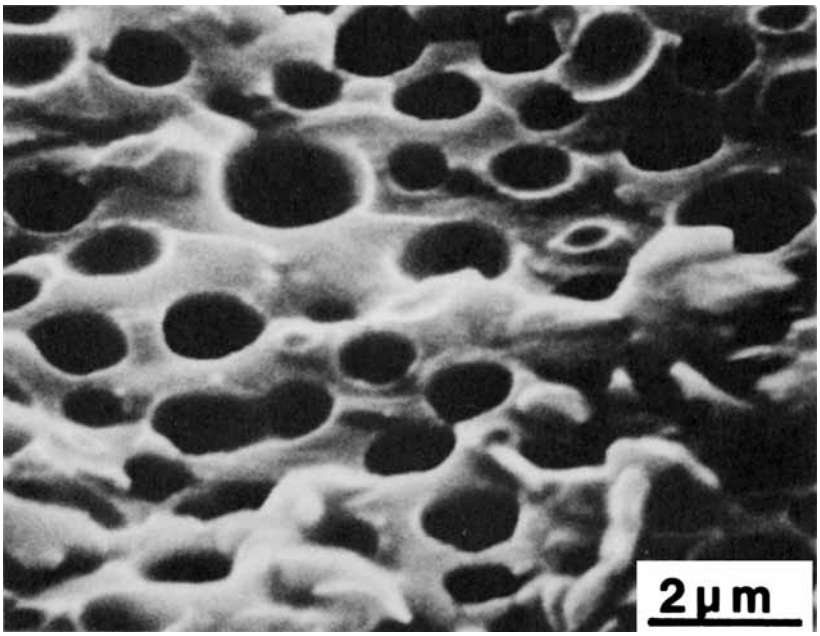

Fig. 5. Fracture surface of the cured model system. The sample was fractured just after being removed from liquid nitrogen (−195°C). The structure of the surface is similar to the one fractured at room temperature.

TABLE I
Density of Resin Systems and DPS

Density (g/cm^3)	Uncured	Cured
Bismaleimide model system, Kerimid FE 70003	1.28	1.17
Bismaleimide formulation without DPS	1.31	1.34
Pure DPS	1.17	1.23

decreases. Thus, it may be assumed that the overall formulation swells during cure, while the individual separate components shrink. The density values of Table I support the cavity formation hypothesis since they suggest approximately a 10% void volume in the cured system.

For further investigation of the morphology of the model resin, experiments were performed in order to identify the DPS in relation to the cavities it may have induced. Figure 6 shows the top of a vertical fracture surface. In addition to the skin effect (a thin layer of 10 μm in thickness without any cavities), it can be seen that, here, each cavity appears to be partially filled with a material surrounding it as a shell. It has to be pointed out that a higher concentration of DPS is expected at the top of the sample, due to the density of DPS which is lower than that of the BMI, allowing migration of DPS to

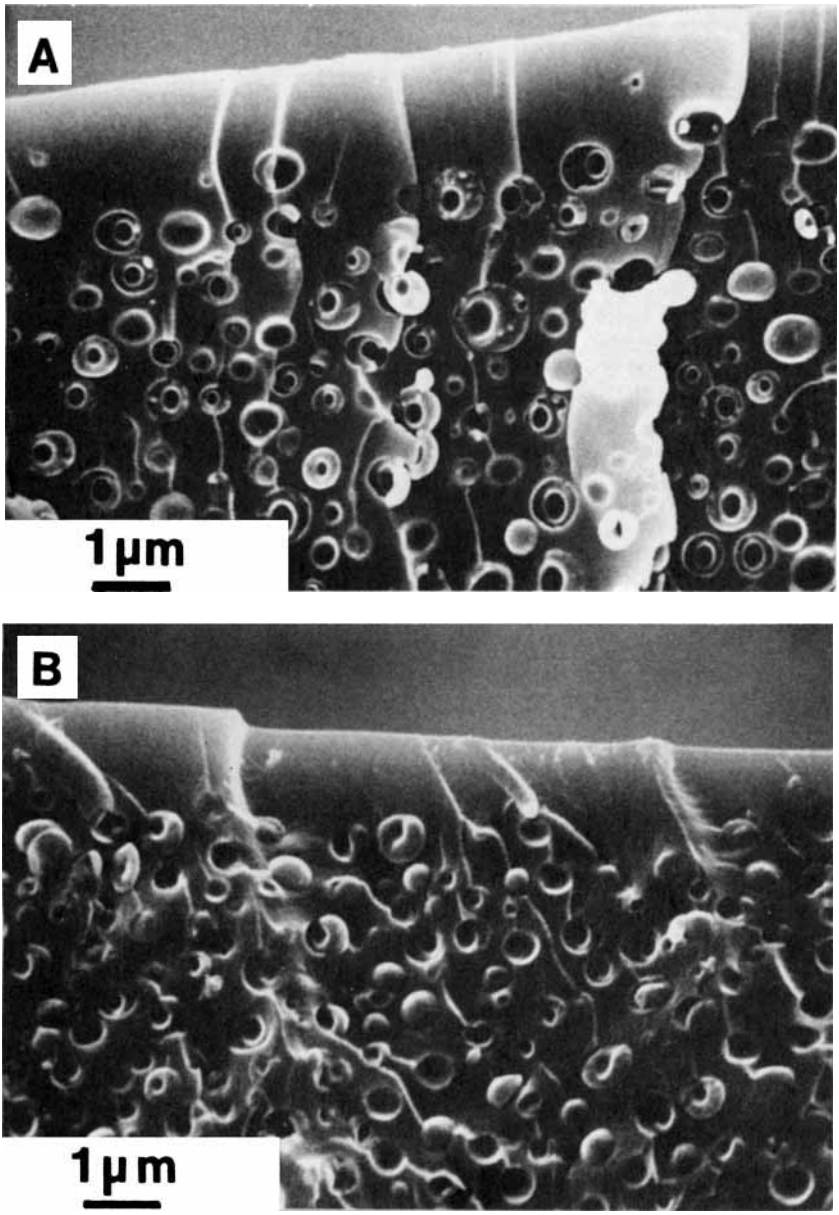

Fig. 6. Part of a fracture surface near the top of a sample cured in a vertical mold. DPS concentration is higher in this area: (a) surface observed just after fracture; (b) surface observed after treatment with DPS swelling solvent hexafluoropropanol for 10 min.

the surface while the formulation is still liquid before gelation. Furthermore, if the fractured sample is immersed into hexafluoropropanol, the material observed in the cavities swells, as shown by Figure 6(b). This observation suggests that these observed shells may contain a higher concentration of DPS than the surrounding material which does not swell in hexafluoropropanol. Shells can also be distinguished around some of the cavities on the fracture surface of Figure 3, where the sample was not exposed to the solvent. However, these shells are much thinner and the boundary

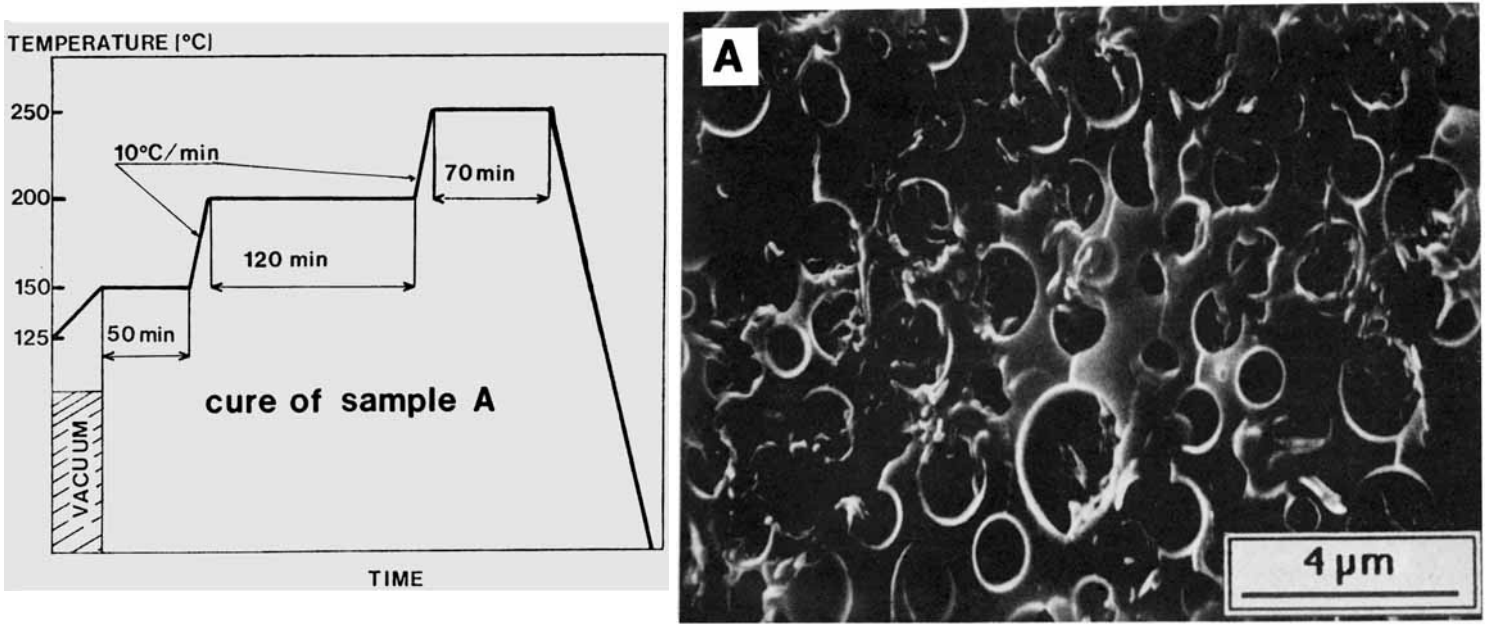

Fig. 7. Distinct morphologies obtained with two different processing conditions: (a) rough heterogeneities partially filling the cavities; (b) no heterogeneities are detectable, smooth shells of DPS are assumed to surround the cavities.

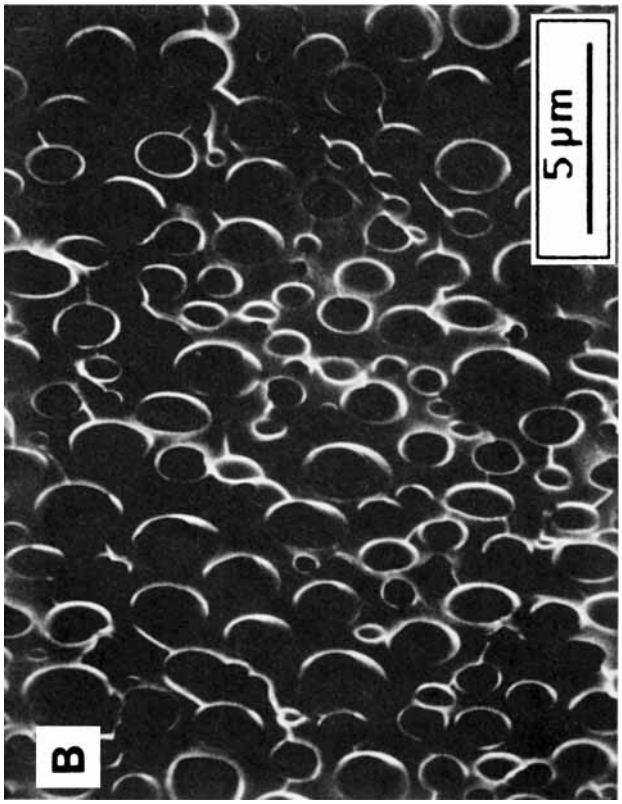

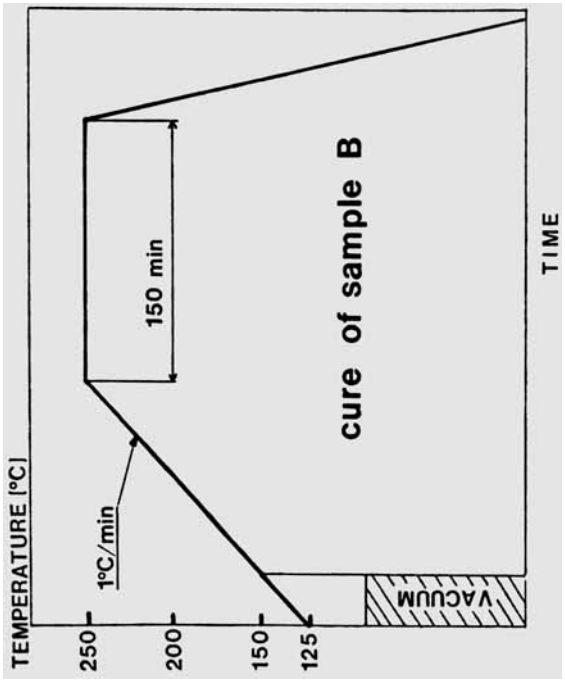

Fig. 7. *(Continued from the previous page.)*

between them and the surrounding resin is not as well defined. Different types of heterogeneities due to DPS were obtained by changing the processing conditions, even though the formed cavities remained equivalent in size and concentration in all samples irrespective of the processing conditions. Figures 7(a) and 7(b) presents two extreme types of morphology, due to two different processing conditions. Specifically, a cure similar to the basic one but with increased heating rates between the plateaus (10°C/min instead of 5°C) gave rough heterogeneities partially filling the cavities (sample A); a 150-min plateau at 250°C following a slow ramp of temperature at 1°C/min apparently gave empty cavities with no detectable surrounding shells (sample B). The morphology obtained with the reference cure cycle, empty cavities surrounded with detectable thin shells, is midway between these two processing induced morphologies.

The observed morphological features (shells or heterogeneities) reveal a phase separation between two materials with different concentrations of DPS. Furthermore, two extreme mechanisms for this phase separation can be proposed, depending on the cure conditions:

A. A "rough" precipitation of excess DPS as the BMI crosslinks while a certain amount of DPS may remain in solution in the BMI network, or even be included in the network if any reaction occurs between the two polymers.[2]

B. A "smooth" separation between the same materials, but here the excess DPS precipitates slowly and no well-defined boundary exists between the BMI network and the precipitated DPS; as a result, the DPS is smoothly distributed against the wall of the cavity in a thin "shell." A gradient of concentration in DPS is assumed from the resin to the cavity.

The conditions prevailing during the reference cure cycle are closer to the second cure variation, giving rise to a "smooth" separation. However, shells may be observed around the cavities.

In summary, the morphology of the cured model bismaleimide resin examined may be viewed as made up by non-communicating cavities (closed porosity) of 1.5 μm in diameter occupying about 10% of the entire volume. Part of the DPS is located in the BMI network (in solution or reacted); and the excess precipitates into thin shells surrounding the cavities. These features are a result of DPS inclusion and may vary with the processing conditions used during the cure.

Development of the Morphology during the Cure

In order to correlate the formation of this morphology to any physicochemical change the resin undergoes during its cure, it is essential to be able to locate precisely the time of cavity initiation as well as growth during the cure.

Real time observation of the formation of the cavities by optical microscopy revealed their sudden onset at a point always located within the first 10 min of the second plateau of temperature at 200°C (see Fig. 2 describing the cure cycle). In the optical microscope setup used, the first cavities appeared at the center of the drop sprayed on the glass slide. Then the area they occupied grew quickly towards the edges. In less than 3 min, the cavities were present in the entire sample. A clear identification of the cavities required examination of a region close to the edge where the sample was thinner. Figure 8

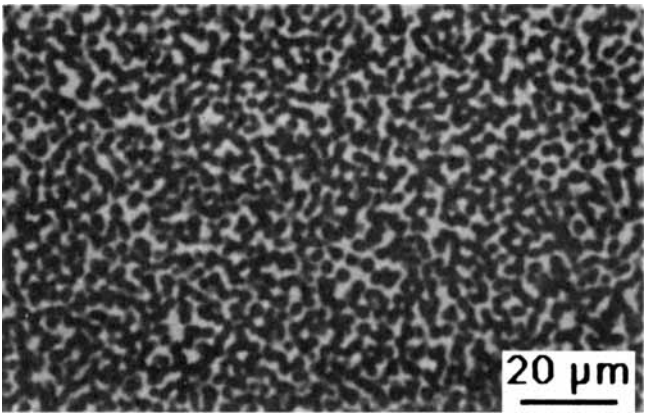

Fig. 8. Transmission optical microscopy on a thin cured sample. Cavities appear as spheres 2 μm in diameter.

shows a part of the sample where only one or two "layers" of cavities are observable through the thickness. The cavities can be seen as small spheres about 2 μm in diameter.

Cavity, as well as void, formation during cure is often associated with emission of volatile products.[14-16] Figure 9 shows thermogravimetric scans at 5°C/min on each major component of the model formulation as well as their combinations. From these plots, it is obvious that some of these components are able to emit high amounts of volatile products at temperatures within the cure range (TAIC and DPS especially). Thermogravimetry (TGA) is also used here specifically to determine whether volatile products remain trapped in the cavities at the time of their formation. It should be pointed out that neither cured BMI formulation without DPS nor pure cured DPS present any cavities. Thus, if the mechanism for the formation of cavities involves emission of volatile products, the cavities may be created by gases that would be able to escape from these two components when cured separately but would remain trapped in the blended formulation. Furthermore, it was observed that the viscosity of the DPS-containing BMI formulation is lower than that of the non-DPS-containing formulation, with both systems gelling at about the same time in the cure cycle. On the other hand, DPS is liquid during the entire cure and solidifies only in the final part of the cooling ramp. As a consequence, some gases may escape more easily from the DPS-containing system than from the non-DPS one. Furthermore, the volatiles trapped in the former may have been emitted by the DPS when the viscosity of the gelling blend is too high to let them escape. Accordingly, the temperature profile of the cure cycle was simulated in the TGA cell on samples with no DPS, on pure DPS, and on the BMI model formulation with DPS. The curves of weight loss as a function of time obtained on DPS, $W_D(t)$, and non-DPS-containing formulation, $W_R(t)$, were combined (using a program of file modification available in the DuPont System 9900 software) into a new curve, $W_C(t)$:

$$W_C(t) = 0.25W_D(t) + 0.75W_R(t) \quad (1)$$

where $W_D(t)$ is the curve obtained by TGA on pure DPS [Fig. 10(c)], $W_R(t)$ is

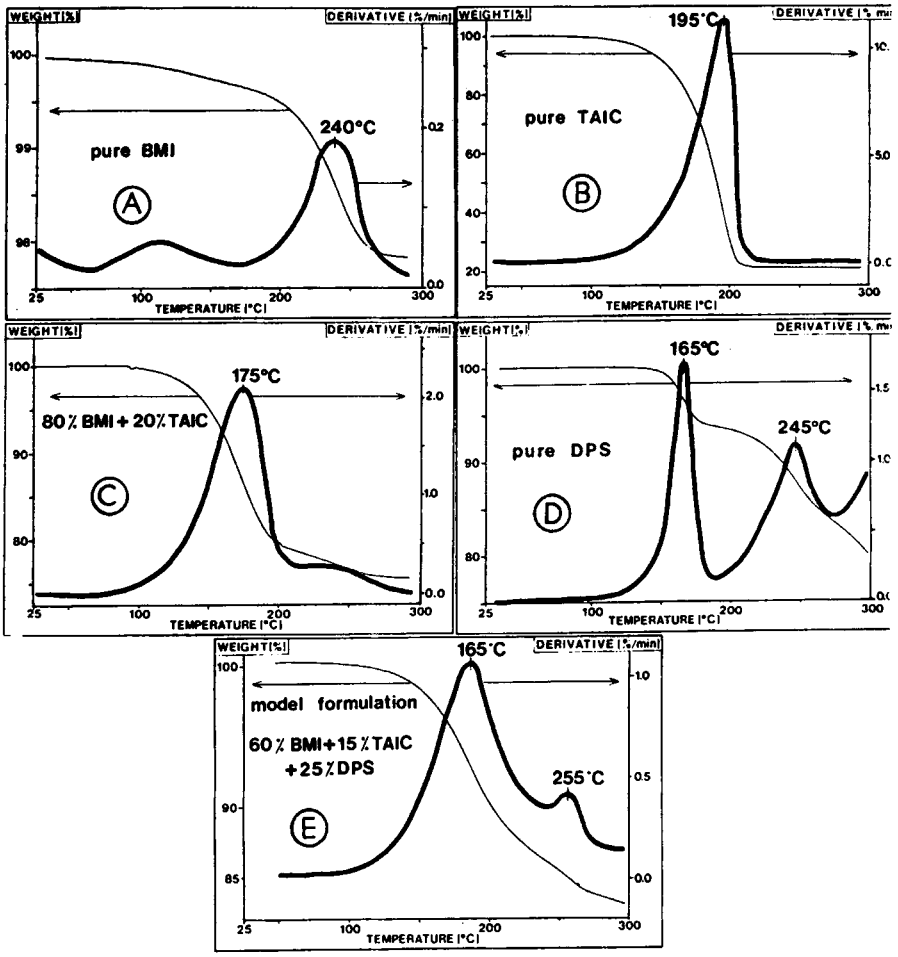

Fig. 9. TGA results on the major components (and their combinations) of the model system scanned at 5°C/min: (a) pure BMI; (b) pure TAIC; (c) 80% BMI + 20% TAIC; (d) pure DPS; (e) final formulation: 60% BMI + 15% TAIC + 25% DPS.

the curve obtained by TGA on formulation without DPS [Fig. 10(b)], and $W_C(t)$ is the calculated curve that would be obtained on an ideal blend, with no physicochemical interactions between its components. The subtraction of this curve from that obtained on the real blended formulation, $W_F(t)$, gives $D(t)$:

$$D(t) = W_F(t) - W_C(t) \tag{2}$$

$$D(t) = W_F(t) - [0.25W_D(t) + 0.75W_R(t)] \tag{3}$$

where $W_F(t)$ is the curve obtained by TGA on the real blended formulation [Fig. 10(a)] and $D(t)$ is the calculated curve of the differences in loss of weight between the virtual ideal blend and the real one [Fig. 10(d)].

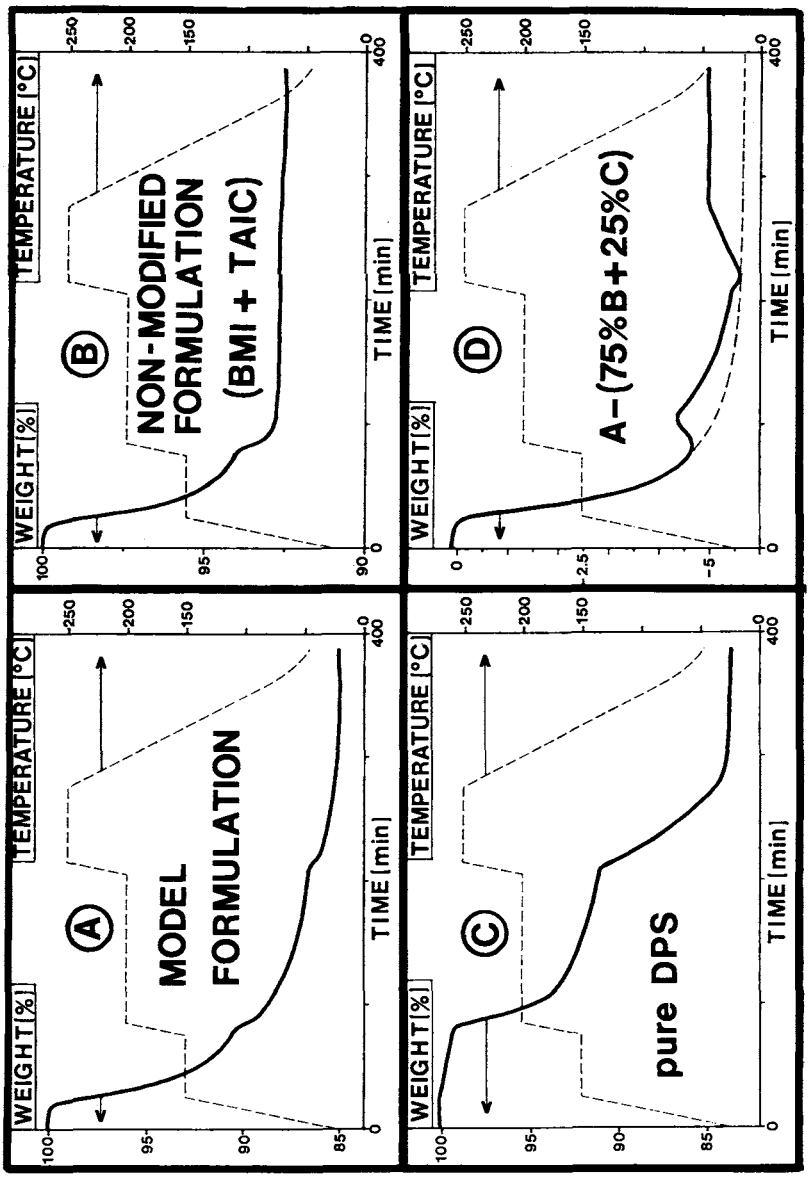

Fig. 10. Simulation of the temperature profile of the cure cycle in a TGA cell on: (a) basic model system; (b) 80% BMI + 20% TAIC; (c) pure DPS; (d) calculated difference between an ideal (60% BMI + 15% TAIC + 25% DPS without any physicochemical interaction) and the basic model formulation.

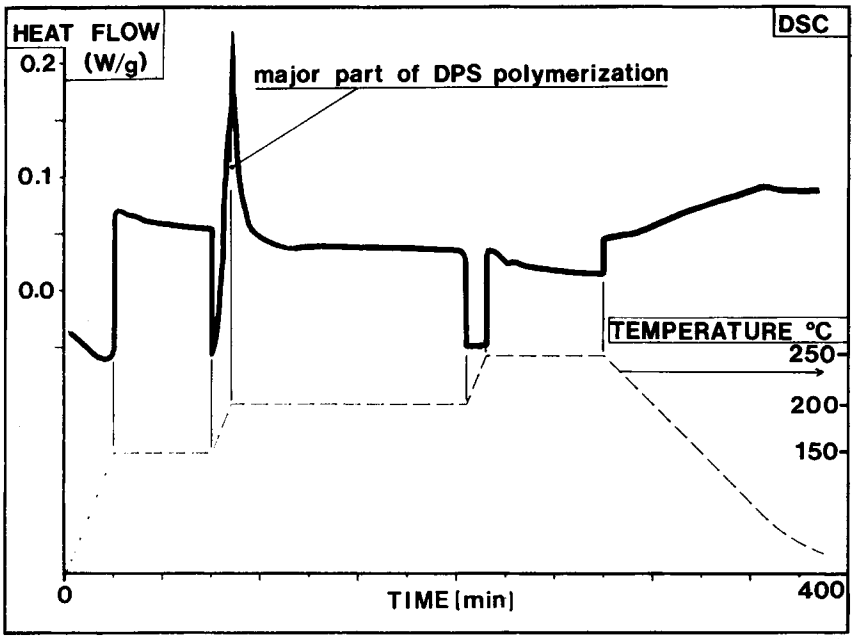

Fig. 11. Simulation of the temperature profile of the cure cycle on pure DPS in a DSC cell. The completion of the DPS polymerization during the 200°C plateau is shown.

The "difference" curve $D(t)$ indicates the departure of a gas from the DPS-containing-system all along the cycle that leaves less easily the formulation without DPS. This evolution is attributed to TAIC, which is the only component of the system without DPS giving rise to a significant loss of weight (Fig. 9). More interestingly, the slope of the calculated curve $D(t)$ turns positive between the first two plateaus of temperature. This may be explained by the existence of volatiles emitted by DPS that would be trapped in the curing resin. A DSC experiment shown in Figure 11 performed on pure DPS by simulating again the cure cycle shows that DPS indeed polymerizes at this time of the cure. Water vapor is the byproduct of this polycondensation in the proportion of 8% in weight of DPS for a complete polymerization. The trapped gas detected here may be assumed to be water vapor. Following this phenomenon, the slope of the "difference" curve $D(t)$ turns negative, again suggesting a slow diffusion of this gas through the sample. A baseline may be extrapolated from the first trend of the $D(t)$ curve [dotted line in Fig. 10(d)]. At the beginning of the last plateau of temperature, the curve tends to join again this baseline, indicating that all the trapped water vapor would have diffused and evaporated from the resin, before the slope turns positive again. This latter trend can be attributed to another gas trapped in the resin. It cannot be assumed to be water vapor since DPS polymerization is complete during the 200°C plateau. However, Figure 10(c) shows that DPS undergoes a high loss of weight during this 250°C plateau. Therefore, it is possible to assume that molecules among the shorter DPS oligomers are lost at that time.

Mechanism for Morphology Creation

Two features of the morphology are of interest here: microcavities and heterogeneities containing a high concentration of DPS. Their formations during the cure of the model resin are interrelated. A mechanism based on the results presented above is thus proposed for the development of the observed morphology.

As the TGA, optical microscopy and SEM results have shown, extensive changes in the morphology start to occur during the ramp between the first two plateaus of the cure cycle: the viscosity increases significantly as the BMI network becomes denser and the excess DPS precipitates into small liquid particles. These particles are too small to be observable by optical microscopy. At the beginning of the 200°C plateau, DPS starts to polymerize, emitting a large amount of water vapor as a byproduct. Since DPS is liquid, the vapor is allowed to gather into bubbles that grow because of the high pressure induced by the vaporization. The high viscosity of the gelling, or even gelled, resin surrounding the DPS prevents the bubbles from moving toward the outside of the sample. At this point, the cavities are initiated. A layer of DPS with a thickness depending on the size of early precipitated particles surround each cavity as a shell. Then, during the rest of the plateau, the vapor can slowly diffuse through the BMI network; and the initial pressure inside the cavities decreases. The increase in density of both DPS and BMI, resulting in their shrinkage, may also help the expansion of the cavities during this part of the cure. Increasing the temperature to 250°C increases the speed of water vapor

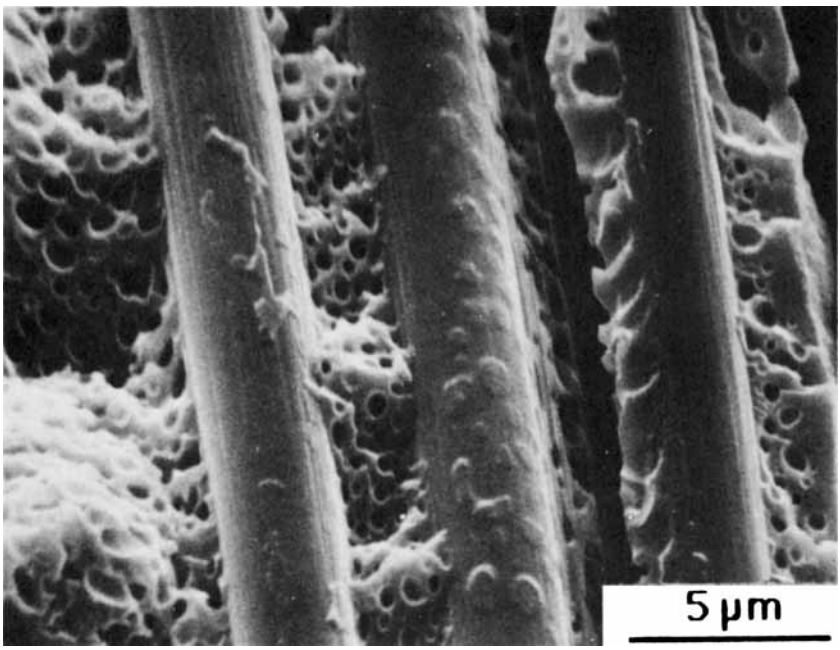

Fig. 12. Interlaminar fracture surface (parallel to the fibers and perpendicular to the ply surface) generated on an unidirectional carbon-fiber-reinforced basic bismaleimide formulation.

diffusion and vaporizes short molecules of DPS; the pressure inside the cavities increases again and the cavities may even expand a little more, making the sample swell. The cooling part of the cycle makes the DPS solidify into a brittle solid. This solidification is accompanied by a shrinkage of the DPS which may let the cavities expand again and decrease their internal pressure. Depending on the amount of DPS present in the cavities as a liquid, it can solidify into either smooth shells around the cavities or rough heterogeneities.

The mechanism explored here is not incompatible with that for an epoxy system. Similar microcavity morphology was described for an epoxy system by Peters and Logan.[17]

Finally, SEM of fractured surfaces shown in Figure 12 for carbon-fiber-reinforced basic model formulation also exhibited the microcavity morphology. This indicates that the presence of the reinforcing fibers does not affect the basic mechanism involved in the creation of the microcavities.

CONCLUSION

A silicone-modified bismaleimide resin has been examined in this work as a model high temperature thermosetting matrix for structural composites. It was established that the silicone additive can induce a morphology for the cured resin similar to those observed on fracture surface of rubber-toughened epoxies. It was demonstrated, however, that the observed noncommunicating microcavities are not created during the fracture process, but during processing as a result of a combination of liquid state of the silicone additive and specific volatile products emission during the cure. Increase in DPS and BMI densities during the cure may also help the cavity expansion.

Collectively, the results of this investigation have provided an important step toward understanding the importance of kinetics of morphology development during processing in order to effectively control the final structure and properties of high temperature matrix-based composite systems.

The authors would like to express their appreciation to Dr. M. Carrega of Rhone-Poulenc for helpful discussions and expert coordination of this project. The invaluable input of the late Dr. M. Rakoutz and his colleagues, Drs. Balme and Barthelemy of Rhone-Poulenc, in chemical formulation issues is also acknowledged. Financial assistance for this project was provided by Rhone-Poulenc, Inc., through the Polymeric Composites Laboratory and in supporting one of the authors (J. F. V.) during a 1-year internship as a Post-Doctoral Research Associate at the Laboratory.

References

1. A. J. Kinloch, S. J. Shaw, and D. A. Tod, in *Rubber-Modified Thermoset Resins*, C. K. Riew and J. K. Gillham, Eds., ACS Series No. 208, Am. Chem. Soc., Washington, DC, 1984, pp. 101–115.

2. G. Pouzols and M. Rakoutz, 30th Natl. SAMPE Symp. Proc., 1985, pp. 606–609.

3. J. C. Seferis and L. Nicolais, Eds., *The Role of the Polymeric Matrix in the Processing and Structural Properties of Composite Materials*, Plenum, New York, 1983.

4. J. C. Seferis, *Polym. Compos.*, **7**, 158 (1986).

5. J. C. Seferis and P. S. Theocaris, Eds., *Interrelations Between Processing, Structure and Properties of Polymeric Materials*, Elsevier, New York, 1984.

6. Rhone-Poulenc, French Pat. No. 83 17218 (1983).

7. D. A. Scola and D. J. Parker, 43rd Annual Tech. Conf. and Exhibit, Soc. Plast. Eng., Inc., ANTEC' 85, April 29–May 5, 1985, Conf. Proc., XXXI, 1985, pp. 399–400.
8. P. Lopez, M. S. thesis, Dept. of Chem. Eng., Univ. of Washington, Seattle, WA, 1985; P. R. Lopez and J. C. Seferis, (1986), in preparation.
9. L. T. Manzione, J. K. Gillham, and C. A. McPherson, *J. Appl. Polym. Sci.*, **26**, 889–906 (1981).
10. L. T. Manzione, J. K. Gillham, and C. A. McPherson, *J. Appl. Polym. Sci.*, **26**, 907–919 (1981).
11. A. F. Yee and R. A. Pearson, *J. Mater. Sci.*, **21**, 2462–2474 (1986).
12. A. F. Yee and R. A. Pearson, *J. Mater. Sci.*, **21**, 2475–2488 (1986).
13. C. B. Bucknall and I. K. Partridge, *Polym. Eng. Sci.*, **26**(1), 54–62 (1986).
14. H.-M. Tong, *Polym. Eng. Sci.*, **25**(2) 75–82 (1985).
15. G. Titomanlio, S. Piccarolo, and G. Marrucci, *Polym. Eng. Sci.*, **25**(2), 91–97 (1985).
16. J. C. Halpin, J. L. Kardos, and M. P. Dudukovic, *Pure Appl. Chem.*, **55**(5), 893–906 (1983).
17. R. A. Peters and T. J. Logan, *Adhesive Age*, (Apr.), (1975).

Received November 13, 1986
Accepted January 15, 1987